https://doi.org/10.17221/163/2025-RAE

A spectral signature-based algorithm for the identifiability of crops and their cultivation conditions

Sarah El Azizi[1], Halima Taia[1], Abdes-Samed Bernoussi[1], Mina Amharref[1], Edyta Wozniak[2]*

[1]*Laboratory CBM-VR, Faculty of Sciences and Techniques, University Abdelmalek Essaadi, Tangier, Morocco*

[2]*Space Research Centre of the Polish, Academy of Sciences, Warszawa, Poland*

**Corresponding author: sarah.elazizi@gmail.com*

Citation: El Azizi S., Taia H., Bernoussi A.-S., Amharref M., Wozniak E. (2026): A spectral signature-based algorithm for the identifiability of crops and their cultivation conditions. Res. Agr. Eng., 72: 59–69.

Abstract: Recent advancements in remote sensing techniques, especially the combination of hyperspectral imaging with analytical algorithms, have greatly improved precision agriculture. This study introduces some algorithms developed for identifying crops and evaluating their growth conditions, focusing on irrigation and fertilisation. The present approach is based on the concept of identifiability of a family of dynamic systems and the differentiation of plants using their spectral signatures. The method uses a repository of spectral data and applies a developed algorithm to compare the measured spectra with the reference database, enabling the identifiability and the recognition of both known and unknown crops. As an application of our approach, we have considered two different crops: mint and rosemary, under different irrigation and fertilisation conditions. The results show that the algorithm achieved a 100% identification rate across the four unknown samples. The minimum spectral distances obtained are 0.01 and 0.03 for rosemary and mint, respectively. Thus, the family of systems was identifiable with a tolerance of $\eta < 0.03$. The study concluded that the algorithm effectively classifies the crop type and deduces its growth conditions, demonstrating its effectiveness for agricultural monitoring.

Keywords: hyperspectral imaging; remote sensing; precision agriculture; plant stress detection; spectral data analysis

Remote sensing technology is essential for efficient agricultural production management, offering a powerful tool for monitoring the distribution of agricultural fields (Campos et al. 2016), for estimating crop yields (Jin et al. 2016), and detecting the effect of water and fertiliser supply for plants (Taia et al. 2024). In fact, as airborne and spaceborne hyperspectral sensors have advanced and become more reliable, this technology is gaining significance and shows great promise for the remote monitoring of vegetation and general agricultural conditions. It captures detailed spectral data about plants, allowing for the detection of their physiological and biochemical states (Adão et al. 2017).

Remote sensing technology is effectively used for plant classification and monitoring of the growth status. Significant progress has been achieved in recent years by integrating hyperspectral technology with algorithms, including support vector machines (SVMs) (Zhong et al. 2022), random forest (RF),

Supported by MESRSI, CNRST and Digital Development Agency (DDA) of Morocco under the projects PPR2 OGI-Env and Al Khawarizmi, Intelligent Management Tool for Irrigation Water and Forestry Heritage.

© The authors. This work is licensed under a Creative Commons Attribution-NonCommercial 4.0 International (CC BY-NC 4.0).

https://doi.org/10.17221/163/2025-RAE

partial least squares regression (PLSR) (Guo et al. 2024), and convolutional neural networks (CNNs) (Tariku et al. 2023). Some of the studies have employed remote sensing modelling for monitoring and enhancing irrigation management around the world (Foster et al. 2019; Venancio et al. 2019). Over the years, numerous research studies have been conducted to investigate and develop effective methods for the identification of plants.

Based on satellite remote sensing, Underwood et al. (2003, 2007) utilised various minimum noise fraction (MNF) techniques derived from AVIRIS hyperspectral imaging data to effectively categorise three non-native plant species located along the coastline of California, utilising maximum likelihood classification (MLC). Senthilnath et al. (2012) chose satellite hyperspectral imagery along with clustering algorithms and classification techniques to effectively detect three developmental phases of wheat plants. Their approach tracked plant growth, resulting in an identification accuracy of 81.5%.

Many studies have used unmanned aerial vehicles (UAVs) to identify and classify plants (Hunt and Daughtry 2018; Tariku et al. 2023). Zhong et al. (2022) coupled UAV-acquired hyperspectral imagery and LiDAR information integrated with SVM. This combination proved to be efficient for identifying tree species in the intricate environment of mixed coniferous and broad-leaved forests. In terms of monitoring the plant growth status, Guo et al. (2024) studied UAV hyperspectral data to analyse the potato growth and leaf water content. They combined spectral mathematical transformations such as multivariate scatter correction (MSC) and standard normal variate (SNV) with classifiers: RF, competitive adaptive reweighted sampling (CARS), support vector regression (SVR) and PLSR. The approach achieved three optimal estimation models: MSC-CARS-SVR, SNV-CARS-PLSR and MSC-RF-PLSR for tuber formation, tuber growth and starch accumulation, respectively. In order to identify leaf spot disease, Anand et al. (2024) utilised spectral reflectance from brinjal (eggplant) leaves across nine different wavelength ranges to train machine learning algorithms, specifically decision tree and SVM. The SVM model reached the highest level of accuracy at 92.4%, successfully classifying more than 99% of the infected tissue and 94% of the healthy tissue, showcasing its capability for accurate monitoring of agricultural diseases. The research led by Yin et al. (2022) shows that deploying hyperspectral sensors on UAVs at various altitudes, along with image classifiers and fusion modelling based on multiple linear regression (MLR) and SVR can effectively and precisely track nitrogen levels in cotton leaves, improving the management of nitrogen fertiliser.

Hyperspectral remote sensing methods based on visible-NIR spectroscopy are among mostly used methods for plant identification owing to the non-destructiveness, non-invasiveness, high-speed, high sensitivity, and specificity. Visible-NIR-SWIR spectroscopy utilises the region spectrum ranging from 400 to 2 500 nm. In this context, the research conducted by El Azizi et al. (2022) shows that UV-NIR field spectroscopy is a powerful tool for tracking the effects of drought on medicinal plants in Northern Morocco, identifying Lavandula stoechas as the most vulnerable to lack of water among the three species examined. Indeed, visible spectroscopy is capable of examining the colour and pigment composition, whereas NIR spectroscopy measures macro components and SWIR assesses the water content. Indeed, pigments, such as chlorophyll, anthocyanin, and carotenes, influence the visible region and could be an indicator for disease and stress detection in plants (Zahir et al. 2022). Remote sensing combined with machine learning has been used to discriminate and identify identical – ecologically and morphologically – plant species. In this context, Pu and Liu (2011) used hyperspectral data measured on the ground to identify 13 species of trees distributed in Tampa by segmented canonical discriminant analysis (CDA), segmented principal component analysis (PCA), segmented stepwise discriminate analysis (SDA), and a segmented maximum likelihood classifier (MLC). With this method, the highest identification accuracy the authors achieved was 96%. Finally, El Azizi et al. (2024) applied principal component analysis (PCA) and partial least squares-discriminant analysis (PLS-DA) to discriminate medicinal and aromatic plant species.

Several concepts have been introduced into systems theory, which are based on the modelling, analysis and control of systems (Pawluszewicz and Molaei 2023; Tripathi et al. 2024). One of these concepts is observability, which consists in being able to reconstruct the state of a given dynamic system whose dynamics are known, through a given

https://doi.org/10.17221/163/2025-RAE

measurement function (Apraiz and Bárcena-Petisco 2023; Tripathi et al. 2024).

If the system is subject to disturbances, it is possible, under certain conditions, to locate them using what are known as spy sensors. Bernoussi et al. (2023) introduced the concept of "identifiability of a family of dynamical systems". We assume a family of models and a measurement function, the hypothesis is the following: can we determine, from the collected measurements, the model of our system knowing that it is in the given family? If we manage to determine it, we will be able to do everything that could be done on a system of which we have both the model and the measurements.

A characterisation for localised dynamical systems is given in (Bernoussi et al. 2023).

In relation to this hypothesis of identifiability and for localised systems, algorithms have been developed to determine which of the dynamical systems in a given family generated the measurements received. Note also that in Bernoussi et al. (2023), both the continuous and discrete cases were considered. In this paper, we have adapted these system identifiability and recognition approaches to the hypothesis of cultivation and growth conditions such as water and nitrogen supply.

Despite the fact that hyperspectral data is frequently collected using airborne or UAV sensors, in this study, it was obtained through field UV-NIR spectroradiometric measurements. These measurements constitute a type of hyperspectral remote sensing and form the foundation of our database. The aim of this work is to develop and validate an algorithm based on a spectral signature capable of identifying both the species of crop and its cultivation conditions (specifically water and fertiliser) using remote sensing data. To achieve this, we adapted the concept of identifiability from systems theory to spectral reflectance data, and we designed a recognition algorithm that matches an unknown spectral sample to its closest reference signature.

MATERIAL AND METHODS

Experimental design and data collection. This study uses spectral signature measurements of two crops – *Mentha spicata* (mint) and *Rosmarinus officinalis* (rosemary) – under various irrigation and fertilisation conditions.

The experimental design aimed to assess the spectrum recognition algorithm in both controlled and real-world contexts. Although measurements of mint and rosemary were conducted in different settings (laboratory, versus field), the goal of the experiment was to assess the spectral recognition method in both controlled and uncontrolled settings. The mint experiments allowed the precise control over irrigation and nutrient levels, isolating their spectral effects. In contrast, rosemary measurements in the field tested the robustness and resilience of spectral signatures under natural variability, focusing solely on irrigation timing. These configurations work together to validate the identifiability and recognition framework in a more comprehensive way. For this reason, the spectral signatures have been taken under natural sunlight for rosemary and under halogen lamp light in laboratory for mint (Figure 1).

The ASD Fieldspec HandHeld spectrometer (Analytical Spectral Devices, Inc., Boulder, CO-USA)

Figure 1. Mint in a pot and rosemary in the field

https://doi.org/10.17221/163/2025-RAE

used in this experiment has a spectral range from 325 to 1 075 nm and a resolution in the very near infrared of approximately 3 nm (around 700 nm). A white reference with a reflectance of around 100% was used for calibration and prior to the measurement of each rosemary sample. The distance between the sensor and the plant considered in this study is 0.35 m.

Since spectral data were collected using a handheld field UV-NIR spectrometer, the reflectance values were radiometrically calibrated, which is consistent with classical spectroradiometric measurement theory. This means that all the measurements and subsequent analyses in this study are strictly based on spectroradiometric acquisition and processing.

All the data were collected and processed using FieldSpec RS3 data-collection software (Ver. 6.4.3, 2008). The Savitzky-Golay filter, which is implemented in Python (Ver. 3.11) with the SciPy library, was used to pre-process the raw spectral data (Virtanen et al. 2020).

Table 1 describes meteorological conditions corresponding to each day of data collection. Since the mint spectral signatures were taken in the laboratory, the wind speed and direction were not considered.

Crop conditions and database construction. The spectral database consists of 18 known crop samples and known conditions (S1 to S18), combining mint samples under 9 different irrigation and fertilisation conditions and rosemary samples measured under 9 different watering contexts. Table 2 illustrates all the detailed conditions for each sample.

Identifiability and algorithm method. Let us consider a family of crops growing under different conditions. For each crop, we collect a measurement – its spectral signature – using a spectrometer.

Denote B as the set of all the obtained spectral signatures Si, for $1 \leq i \leq n$, for each crop under particular growth conditions, where n is the number of spectral signatures in our family of systems.

We have:

$$B = \{Si(y), 1 \leq i \leq n\} \quad (1)$$

The considered hypotheses are:

(P) For an obtained measurement (spectral signature) of an unknown (or known) crop, but where the conditions of its cultivation (water/fertiliser) are not known, can we determine:
- The type or the species of the culture which gave the distinctive spectral signature;
- The conditions of its cultivation?

These hypotheses lead us to another question linked to the reference database and which is:

For the database constituted for the family of systems (spectral signatures of cultures), in each sense can we consider this database reliable?

The approach to these hypotheses is based on the concept of identifiability of families of systems, recently introduced by Bernoussi et al. (2023). For this, we adapt the concept of identifiability to our case. Then we developed a suitable algorithm based on the infinity Norm Method (Gallouêt and Herbin 2011).

Table 1. Meteorological conditions for the day of data collection from the mint in the laboratory and for rosemary under natural light

Sample	Wind speed (km·h^{-1})	Temperature (°C)	Wind direction	Cloud cover (%)
S1 to S9	–	27	–	23
S10	24	23	south-west	28
S11	25	23	south-west	35
S12	17	20	south	35
S13	25	23	south-west	10
S14	22	26	south-west	15
S15	26	23	south-west	14
S16	20	19	west	75
S17	6	19	south-west	75
S18	9	19	west-south-west	75

https://doi.org/10.17221/163/2025-RAE

Table 2. Database used in the identifiability study

Sample	Culture	Conditions
S1	mint	no irrigation and no added nutrients
S2	mint	irrigated with 75% of the optimum amount of water
S3	mint	irrigated with an optimal amount of water
S4	mint	irrigated with 125% of the optimum amount of water
S5	mint	irrigated with the optimum amount of water and with 75% of the optimum amount of nutrient added
S6	mint	irrigated with the optimum amount of water and with the optimum amount of nutrient added
S7	mint	irrigated with the optimum amount of water and with 125% of the optimum amount of nutrient added
S8	mint	irrigated with 75% of the optimum amount of water and with 75% of the optimum amount of nutrient added
S9	mint	irrigated with 125% of the optimum amount of water and with 125% of the optimum amount of nutrient added
S10	rosemary	without irrigation
S11	rosemary	after one day without irrigation
S12	rosemary	after four weeks without irrigation
S13	rosemary	24 h after the first irrigation
S14	rosemary	24 h after the second irrigation
S15	rosemary	24 h after the third irrigation
S16	rosemary	after 24 hours of intensive irrigation
S17	rosemary	after four days of irrigation
S18	rosemary	after seven days of irrigation

Identifiable family of systems/cultures and reliability of the database

We consider a family of dynamic systems describing different measurements subjected to different crops and growth conditions (water/fertiliser). The measurement function in our case is given by a wavelength spectrometer in a given interval $[\lambda_0, \lambda_f]$. The measurement is represented by a spectral signature $Si(\lambda)$; $\lambda \in [\lambda_0, \lambda_f]$.

Specifying the state of each crop is noted $Z(t)$ and the measure function is given via a spectrometer which gives us the spectral signature, noted Si, for $i = 1, n$, where n is the number of spectral signatures in the database.

We have the following definition:

Definition 3.1. The family of culture with different conditions, is identifiable (for spectrometer) if for any two different cultures with different conditions the measure gives two different spectral signatures, i.e., Si and Sj satisfying $Si(.) \neq Sj(.)$ in $[\lambda_0, \lambda_f]$.

We say that the database obtained from the family of systems (culture) is reliable if the corresponding family is identifiable.

We have the following remark:

Remark 3.2. Mathematically speaking, $Si(.) \neq Sj(.)$ in $[\lambda_0, \lambda_f]$, means that there exists at least $\lambda \in [\lambda_0, \lambda_f]$ such that $Si(\lambda) \neq Sj(\lambda)$. However, in practice $Si(.) \neq Sj(.)$, means that $d(Si(.), Sj(.)) \geq \eta > 0$ where $d(Si(.), Sj(.))$ is a given distance between the two spectral signatures $Si(.)$ and $Sj(.)$.

So, we can define the family identifiability according to a given distance and a threshold η depending on the nature of the sensor used to collect the measurements (spectral signature in this case).

To characterise the identifiable family, we consider a chosen distance, between two given spectral signatures, noted ds noted by:

$$ds(S1(.), S2(.)) \quad (2)$$

where: $S1(.)$, $S2(.)$ – two given spectral signatures in the range $[\lambda_0, \lambda_f]$.

Remark 3.3. The value of the distance defined in Equation (2) depends on the nature of the spectrometer used and particularly on the spectral

https://doi.org/10.17221/163/2025-RAE

range $[\lambda_0, \lambda_f]$. We will consider this remark when we will choose particular distance.

Proposition 3.4. Denote B as the database (set of spectral signatures obtained from the considered cultures), then we have for Si, Sj in B , $Si(.) \neq Sj(.)$ if $ds(Si(.), Sj(.)) \geq \eta > 0$

where η is a given (chosen) tolerance (for identifiability). So, for the quality of the database (reliability) we compute:

$$\rho_B = \min\{ds(Si, Sj); Si, Sj \in B, i \neq j\} \quad (3)$$

Proposition 3.5. The family of systems is identifiable if and only if $\rho_B \geq \eta > 0$, where η is a given (chosen) tolerance for accepting results.

In this case, we say that the family of systems is identifiable with tolerance η.

Remark 3.6. Proposition 3.5 means that for all $Si, Sj \in B$, we have $ds(Si, Sj) \geq \rho_B \geq \eta > 0$

So, to verify if a given family of crops growing in different conditions is identifiable through the data set of collected measures (spectral signatures), we consider the following algorithm.

Algorithm 1. Family identifiability:

(1) Choose a convenient threshold $\eta > 0$ which permit to differentiate between two spectral signatures;

(2) Compute $\rho_B = \min ds(Si, Sj)$; $Si, Sj \in B$; $i \neq j$

– If $\rho_B = \min ds(Si, Sj) \geq \eta$; $Si, Sj \in B$ Stop: the family is identifiable;

– Else the family is not identifiable for the considering measure and threshold η.

Stop

Remark 3.7. If the family is not identifiable through the measurements used to collect the spectral signatures, we must change:

– the threshold η;

– or the spectral range $[\lambda_0, \lambda_f]$

As it will be shown in the example/application.

Now if the family is identifiable, we can consider the hypothesis H_1

Algorithm recognising for an unknown culture

We can formulate the hypothesis H1, as:

(P1) For a given unknown spectral signature Sx, determine the nearest spectral signature in B to Sx. For that, we use the nearest neighbour principle.

Algorithm 2. Nearest neighbour in B:

Note ε as the tolerance of accepting the closest spectral signature as a sought signature

(1) Choose a given a tolerance ε

(2) Compute

$$ds(Sx, B) = \min ds(Sx(.), Si(.)) \quad Si \in B \quad (4)$$

– If $ds(Sx(.), B) > \varepsilon$; stop, no acceptable solution!!!

– Else

Determine the "admissible set" of spectral signatures which realise:

$$Aad(Sx) = \{Si \in B: ds(Sx, Si) = ds(sx, B)\} \quad (5)$$

– If $Aad(Sx) = \{Sk\}$, "singleton"; stop: Sk is the solution;

– Else $Aad(Sx) = \{Sk, Sh, Sl, ...\}$

We adjust the wavelength range $[\lambda_0, \lambda_f]$ corresponding to the spectral range and return to step 2;

– If there is a wavelength range in $[\lambda_0, \lambda_f]$ such that $Aad(Sx) = \{Sk\}$, stop Sk is the solution

– Else stop, no solution;

– Stop.

RESULTS

This section introduces the algorithm-based identifiability analysis of the spectral database and the recognition results for the four unknown samples.

Identifiability of a Family of systems and the reliability of the database:

To assess whether different crop conditions could be reliably distinguished using their spectral signatures, we applied a distance-based identifiability approach.

Chosen distance for the database. In this paper we consider the distance given by:

$$ds(S1(.), S2(.)) = \| S1(.) - S2(.) \| \infty = \sup |S1(\lambda) - S2(\lambda)|; \lambda \in [\lambda 0, \lambda f] \quad (6)$$

To compute $\rho_B = \min ds(Si, Sj)$; $Si, Sj \in B$, we calculate

$$ds(Si(.), Sj(.)) = \sup |Si(\lambda) - Si(\lambda)|; \lambda \in [\lambda 0, \lambda f] \quad (7)$$

Regarding Remark 3.7, if we consider Figure 2 and the wavelength range [325, 425] nm, it is clear that the family is not identifiable. In contrast, considering the larger interval [325, 1 025] nm, the family is identifiable.

The database B of spectral signatures: $B = (S1; ...; S18)$ is illustrated in Figure 2.

https://doi.org/10.17221/163/2025-RAE

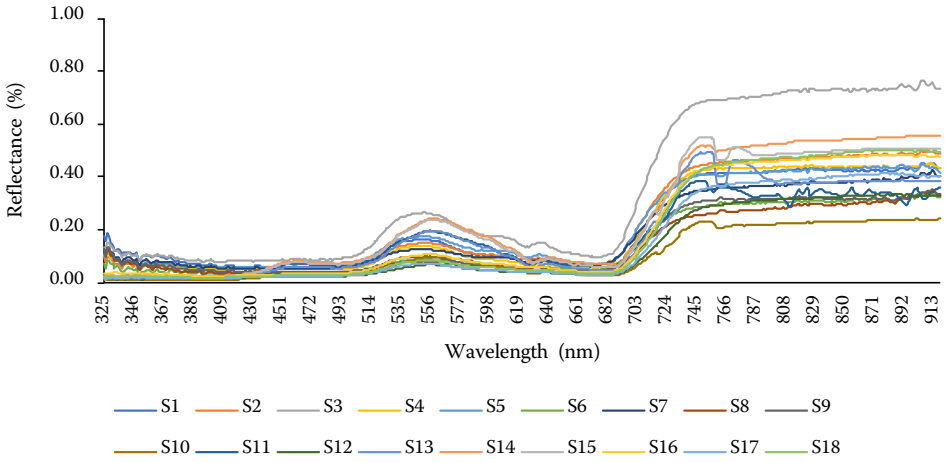

Figure 2. Spectral signatures of the plants in the database *B*

After algorithm application, we obtained the result given in Table 3.

And consequently, we obtain $\rho_B = \min ds(Si, Sj) = 0,03$; $Si, Sj \in B, i \neq j$

Result 4.1. The family of systems (cultures) given through database *B* is identifiable with a tolerance $\eta < 0.03$.

This result is consistent with the qualitative observations.

Recognising an unknown culture:

Principle: By comparing the spectral signature of the four unknown crops *x*, which we called *Sx*,1, *Sx*,2, *Sx*,3 and *Sx*, with unknown water and fertilisation conditions, with the 18 crops in the rosemary and mint database. We determine the spectral signatures of the database *B* closest to the four *Sx* considered. We applied the algorithm. We determine the nearest spectral signature from the database *B* to *Sx*.

Table 3. Maximum value of the differences between the pairwise comparisons of the cultures from the database

S1	S2	S3	S4	S5	S6	S7	S8	S9	S10	S11	S12	S13	S14	S15	S16	S17	S18	Distance
	0.09	0.32	0.07	0.06	0.13	0.06	0.16	0.12	0.21	0.16	0.17	0.16	0.16	0.16	0.15	0.16	0.16	S1
		0.27	0.06	0.08	0.17	0.10	0.19	0.17	0.26	0.19	0.18	0.12	0.10	0.11	0.10	0.15	0.12	S2
			0.32	0.32	0.44	0.36	0.44	0.43	0.53	0.45	0.43	0.38	0.23	0.26	0.28	0.36	0.29	S3
				0.04	0.14	0.08	0.17	0.13	0.22	0.15	0.15	0.09	0.12	0.13	0.07	0.11	0.09	S4
					0.13	0.06	0.15	0.13	0.22	0.15	0.16	0.11	0.14	0.14	0.09	0.14	0.11	S5
						0.09	0.06	0.05	0.12	0.11	0.08	0.20	0.24	0.26	0.17	0.10	0.19	S6
							0.10	0.08	0.18	0.11	0.13	0.14	0.17	0.20	0.10	0.11	0.12	S7
								0.05	0.11	0.13	0.11	0.23	0.26	0.29	0.19	0.12	0.20	S8
									0.12	0.11	0.12	0.18	0.24	0.24	0.17	0.11	0.19	S9
										0.16	0.10	0.26	0.32	0.32	0.25	0.18	0.27	S10
											0.13	0.15	0.26	0.21	0.19	0.12	0.20	S11
												0.21	0.24	0.27	0.15	0.08	0.17	S12
													0.17	0.12	0.10	0.14	0.12	S13
														0.05	0.14	0.17	0.16	S14
															0.13	0.20	0.16	S15
																0.08	**0.03**	S16
																	0.10	S17
																		S18

The value in bold represents the minimum distance among all pairwise comparisons between cultures in the database *B*

https://doi.org/10.17221/163/2025-RAE

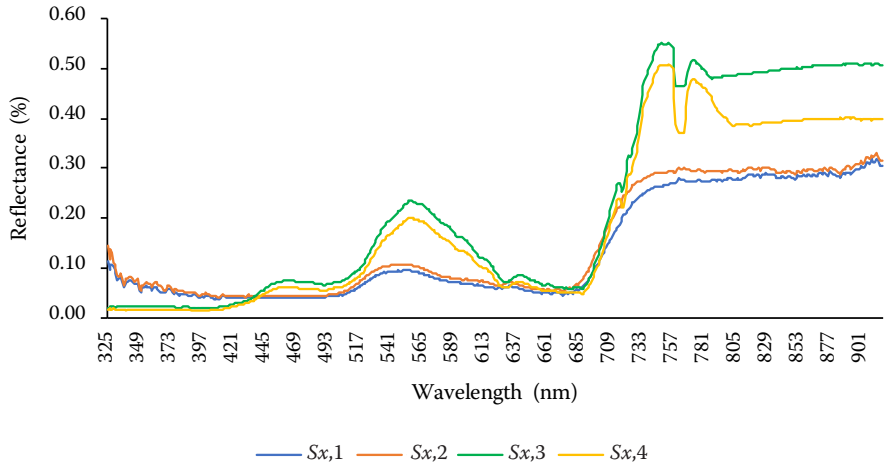

Figure 3. The spectral signatures of the unknown crops

To illustrate this approach, the four unknown crops whose spectral signature *Sx*,1, *Sx*,2, *Sx*,3 and *Sx*,4 are shown in Figure 3.

Table 4 presents the calculation of distance for the Infinity norm method for the four unknown crops. We can observe that the unknown crop *Sx* is similar to the same system within the 18 systems from the database based on the algorithm.

For the unknown crop *Sx*,1:

– The smallest value is 0.03, indicating a spectral similarity between *Sx*,1 and S8.

Spectrum *S*8 is the most similar to the unknown spectrum *Sx*,1. The other spectra have more significant deviations. Note that *Sx*,1 is a mint with optimal irrigation and optimal nutrient addition.

For the unknown crop *Sx*,2:

– The smallest value 0.03, showing spectral similarity between *Sx*,2 and *S*9.

Spectrum *S*9 is the most similar to the unknown spectrum *Sx*,2. The other spectra have more significant deviations. So, *Sx*,2 is a mint with an over-irrigation of 125% of the optimal amount of water and an addition of 125% of the optimal amount of nutrient.

For the unknown crop *Sx*,3:

– The smallest value 0.01, showing spectral similarity between *Sx*,3 and *S*15.

Spectrum *S*15 is the most similar to the unknown spectrum *Sx*,3. So, *Sx*,3 is an irrigated rosemary close to *S*15 which correspond to rosemary 24 h after a third irrigation.

For the unknown crop *Sx*,4:

– The smallest value 0.01, showing the spectral similarity between *Sx*,4 and *S*13.

Spectrum *S*13 is the most similar to the unknown spectrum *Sx*,4. Thus, *Sx*,4 is an irrigated rosemary close to *S*13, which corresponds to rosemary 24 h after the first irrigation.

Figure 4 shows the spectral signatures of the plants in the database and the spectral signatures of the unknown crops. Visually, the structure of the curve for the unknown plant (red) is similar to the

Table 4. Calculation of the similarity of the unknown reflectance spectrum *Sx*,1, *Sx*,2, *Sx*,3 and *Sx*,4 with the 18 spectra in the database

Distance	S1	S2	S3	S4	S5	S6	S7	S8	S9	S10	S11	S12	S13	S14	S15	S16	S17	S18	Closest match
Sx,1	0.15	0.20	0.46	0.16	0.16	0.05	0.11	**0.03**	0.05	0.11	0.12	0.10	0.23	0.27	0.29	0.20	0.13	0.22	0.03
Sx,2	0.14	0.19	0.45	0.15	0.15	0.08	0.10	0.04	**0.03**	0.13	0.12	0.13	0.20	0.26	0.26	0.19	0.13	0.21	0.03
Sx,3	0.16	0.11	0.26	0.13	0.14	0.26	0.20	0.29	0.24	0.32	0.21	0.27	0.13	0.05	**0.01**	0.13	0.20	0.15	0.01
Sx,4	0.16	0.11	0.37	0.09	0.11	0.22	0.16	0.25	0.20	0.28	0.16	0.22	**0.01**	0.16	0.11	0.09	0.16	0.12	0.01

The values shown in bold correspond to the minimum distance between each unknown reflectance spectrum *Sx*,*i* and the reference spectra *Sj* in the database

https://doi.org/10.17221/163/2025-RAE

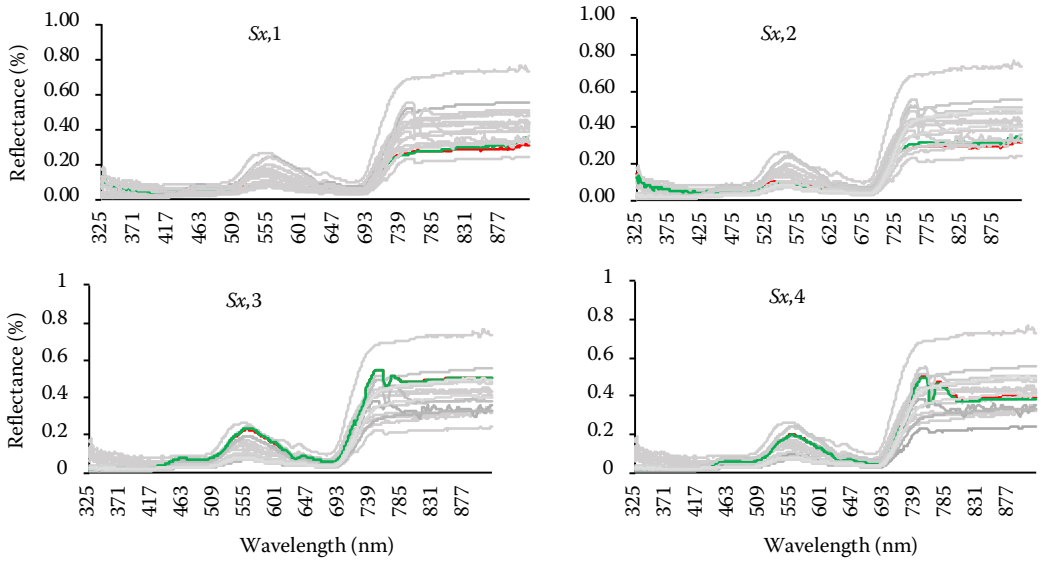

Figure 4. Spectral signatures of the plants in the database and the unknown crops

structure of the curve for the closest crop (green) calculated using our algorithm, and the reflectance values for the two plants are also closer than for the other plants.

After identifying *Sx*,1, *Sx*,2, *Sx*,3 and *Sx*,4, the results obtained showed the reliability of the similarity methods chosen. In fact, the spectral signatures of the crops chosen at the beginning of the demonstration, which were assumed to be unknown, are known and are chosen from the mint and rosemary database in another measurement protocol. This second protocol takes into account two pots for each irrigation and fertilisation situation. The database then contains mint and rosemary in pots from different situations (see Table 1) and the four unknown crops (hypothesis) are chosen from the other remaining mint and rosemary pots, each of which has a pot from the same situation in the database for confirmation of our study, as shown in Table 5.

DISCUSSION

In this study, we have developed a novel and effective algorithm to identify four crops and their growth conditions based on field spectral signatures and a fixed tolerance $\eta < 0.03$. This demonstrates that a single distance-based algorithm can show high accuracy when applied to carefully collected spectral data. Examining other works, Pu and Liu (2011) used complex statistical techniques to separate 13 tree species using hyperspectral data and CDA. While Yin et al. (2022) applied multiple linear regression to UAV-based hyperspectral images for nitrogen monitoring over large areas, obtaining $R = 0.96$. However, their method

Table 5. Four unknown crops with growing conditions

Unknown spectrum	*Sx*,1	*Sx*,2	*Sx*,3	*Sx*,4
Nearest spectral signature to *Sx*	*S*8	*S*9	*S*15	*S*13
True crop	mint	mint	rosemary	rosemary
Conditions	irrigated with the optimum amount of water and with an optimum addition of nutrient	irrigated with 125% of the optimal amount of water and with 125% of the optimal amount of nutrient added	24 h after the first irrigation	24 h after the third irrigation
Correct classification	yes	yes	yes	yes

https://doi.org/10.17221/163/2025-RAE

Table 6. Summary of the comparative results

Study	Main goal	Data type	Model	Accuracy	Complexity
This study	crops/growth conditions identifiability	field spectral data/ spectrometer	infinity norm distance $\eta < 0.03$	100% (4/4 samples correctly classified)	low/easy interpretation
Pu and Liu (2011)	identify tree species	field spectral data	CDA	not quantified/ effective	high
Jin et al. (2016)	predict biomass/ yield	field hyperspectral data	RMSE ~0.72 t·ha^{-1}	simulation and regression	high
Yin et al. (2022)	estimate leaf nitrogen	hyperspectral data from UAV	$R^2 = 0.96$; RMSE = 1.12	MLR	moderate
Tariku et al. (2023)	plant identification	RGB from UAV	90%	deep learning (CNN)	high

CDA – canonical discriminant analysis; RMSE – root mean square error; UAV – unmanned aerial vehicle; MLR – multiple linear regression; CNN – convolutional neural network

targets continuous features and requires more complex modelling. Tariku et al. (2023) obtained an accuracy of almost 90% using UAV and CNN deep learning computing; their approach is less sensitive to small spectral changes. Finally, Jin et al. (2016) used field spectral data combined with a crop model called AquaCrop and achieved RMSE = 0.72 t·ha^{-1}, focusing more on prediction than classification. Table 6 summarises the key insights of each study.

Our algorithm uses distance-based spectral comparison to reach accurate identification (100%), in comparison with the study of Tariku et al. (2023), based on machine-learning approaches, which depend on large training datasets. Furthermore, our method achieves optimal classification using the infinity norm and does not require dimensionality reduction. In contrast to Pu and Liu (2011), who employed multiple statistical models to attain 96% accuracy across tree species.

CONCLUSION

In this study, we developed and applied an algorithm to identify crops and assess their irrigation and fertilisation conditions using hyperspectral remote sensing. We focused on two crops: mint (*Mentha spicata*) and rosemary (*Rosmarinus officinalis*), and constructed a database from controlled and uncontrolled settings, measuring their spectral responses under varying water and fertiliser conditions.

The reliability of the spectral signatures was confirmed by demonstrating that the database could be identified with a tolerance $\eta < 0.03$. With 100% accuracy, the algorithm using the infinite norm identified each of the four unknown samples and their corresponding growth conditions. The method's potential to find useful applications in precision agriculture was demonstrated by its robustness in both controlled (mint) and uncontrolled (rosemary) environments.

Looking ahead, extending this work to include temporal monitoring of crop development would allow for the dynamic modelling of growth stages and yield prediction. Achieving this will require a more comprehensive database, gathered through future laboratory and field campaigns. Developing such a dataset would not only improve our understanding of how crops respond to different irrigation and fertilisation strategies over time, but also contribute to more informed decision-making in precision agriculture. This next phase of research is under consideration.

REFERENCES

Adão T., Hruška J., Pádua L., Bessa J., Peres E., Morais R., Sousa J.J. (2017): Hyperspectral imaging: A review on UAV-based sensors, data processing and applications for agriculture and forestry. Remote Sensing, 9: 1110.

Anand R., Parray R.A., Mani I., Khura T.K., Kushwaha H., Sharma B.B., Sarkar S., Godara S. (2024): Spectral data driven machine learning classification models for real time leaf spot disease detection in brinjal crops. European Journal of Agronomy, 161: 127384.

Apraiz J., Bárcena-Petisco J.A. (2023): Observability and control of parabolic equations on networks with loops. Journal of Evolution Equations, 23: 37.

https://doi.org/10.17221/163/2025-RAE

Bernoussi A., Wozniak E., Belfekih A. (2023): Identifiability of a family of dynamical systems: Application to crops identification. Advances in Systems Science and Applications, 23: 119–147.

Campos-Taberner M., García-Haro F.J., Confalonieri R., Martínez B., Moreno Á., Sánchez-Ruiz S., Gilabert M.A., Camacho F., Boschetti M., Busetto L. (2016): Multitemporal monitoring of plant area index in the Valencia rice district with PocketLAI. Remote Sensing, 8: 202.

El Azizi S., Amharref M., Bernoussi A.S. (2022): Study of drought effects on three medicinal and aromatic plants using field spectroscopy. Journal of Ecological Engineering, 23: 155–162.

El Azizi S., Amharref M., Es-Saouini H., Bernoussi A.S., El Abdellaoui J.E. (2024): Towards a spectral library of medicinal and aromatic plant species (MAPs): Plant discrimination and wavelength selection. Microchemical Journal, 207: 111854.

Foster T., Gonçalves I.Z., Campos I., Neale C.M.U., Brozović N. (2019): Assessing landscape scale heterogeneity in irrigation water use with remote sensing and in situ monitoring. Environmental Research Letters, 14: 024004.

Gallouët T., Herbin R. (2011): Analyse numérique des équations aux dérivées partielles. Master Lecture Notes, Université d'Aix-Marseille, France.

Guo F., Feng Q., Yang S., Yang W. (2024): Estimation of potato canopy leaf water content in various growth stages using UAV hyperspectral remote sensing and machine learning. Frontiers in Plant Science, 15: 1458589.

Hunt Jr, E.R., Daughtry C.S.T. (2018): What good are unmanned aircraft systems for agricultural remote sensing and precision agriculture? International Journal of Remote Sensing, 39: 5345–5376.

Jin X., Kumar L., Li Z., Xu X., Yang G., Wang J. (2016): Estimation of winter wheat biomass and yield by combining the AquaCrop model and field hyperspectral data. Remote Sensing, 8: 972.

Pawluszewicz E., Molaei M.R. (2023): On the notion of observers. Journal of Dynamical and Control Systems, 29: 1855–1865.

Pu R., Liu D. (2011): Segmented canonical discriminant analysis of in situ hyperspectral data for identifying 13 urban tree species. International Journal of Remote Sensing, 32: 2207–2226.

Senthilnath J., Omkar S.N., Mani V., Karnwal N., Shreyas P.B. (2012): Crop stage classification of hyperspectral data using unsupervised techniques. IEEE Journal of Selected Topics in Applied Earth Observations and Remote Sensing, 6: 861–866.

Taia H., Bernoussi A.S., Wozniak E., Amharref M., El Azizi S. (2024): Using hyperspectral reflectance to evaluate the impact of irrigation and fertilization on mint. Agronomy Research, 22: 1312–1323.

Tariku G., Ghiglieno I., Gilioli G., Gentilin F., Armiraglio S., Serina I. (2023): Automated identification and classification of plant species in heterogeneous plant areas using unmanned aerial vehicle-collected RGB images and transfer learning. Drones, 7: 599.

Tripathi M., Moysis L., Gupta M.K., Fragulis G.F., Volos C. (2024): Observer design for nonlinear descriptor systems: A survey on system nonlinearities. Circuits, Systems, and Signal Processing, 43: 2853–2872.

Underwood E., Ustin S., DiPietro D. (2003): Mapping nonnative plants using hyperspectral imagery. Remote Sensing of Environment, 86: 150–161.

Underwood E.C., Ustin S.L., Ramirez C.M. (2007): A comparison of spatial and spectral image resolution for mapping invasive plants in coastal California. Environmental Management, 39: 63–83.

Venancio L.P., Mantovani E.C., do Amaral C.H., Neale C.M.U., Gonçalves I.Z., Filgueiras R., Campos I. (2019): Forecasting corn yield at the farm level in Brazil based on the FAO-66 approach and soil-adjusted vegetation index (SAVI). Agricultural Water Management, 225: 105779.

Virtanen P., Gommers R., Oliphant T.E., Haberland M., Reddy T., Cournapeau D., Burovski E., Peterson P., Weckesser W., Bright J., van der Walt S.J., Brett M., Wilson J., Millman K.J., Mayorov N., Nelson A.R.J., Jones E., Kern R., Larson E., Carey C.J., Polat I., Feng Y., Moore E.W., VanderPlas J., Laxalde D., Perktold J., Cimrman R., Henriksen I., Quintero E.A., Harris C.R., Archibald A.M., Ribeiro A.H., Pedregosa F., van Mulbregt P., SciPy 1.0 Contributors (2020): SciPy 1.0: Fundamental algorithms for scientific computing in Python. Nature Methods, 17: 261–272.

Yin C., Lv X., Zhang L., Ma L., Wang H., Zhang L., Zhang Z. (2022): Hyperspectral UAV images at different altitudes for monitoring the leaf nitrogen content in cotton crops. Remote Sensing, 14: 2576.

Zahir S.A.D.M., Omar A.F., Jamlos M.F., Azmi M.A.M., Muncan J. (2022): A review of visible and near-infrared (Vis-NIR) spectroscopy application in plant stress detection. Sensors and Actuators A: Physical, 338: 113468.

Zhong H., Lin W., Liu H., Ma N., Liu K., Cao R., Wang T., Ren Z. (2022): Identification of tree species based on the fusion of UAV hyperspectral image and LiDAR data in a coniferous and broad-leaved mixed forest in Northeast China. Frontiers in Plant Science, 13: 964769

Received: September 26, 2025
Accepted: December 16, 2025
Published online: February 9, 2026